Engineering N-terminal domain of tissue inhibitor of metalloproteinase (TIMP)-3 to be a better inhibitor against tumour necrosis factor-α-converting enzyme

Meng-Huee LEE*[1], Vandana VERMA*, Klaus MASKOS†, Deepa NATH*, Vera KNÄUPER‡[2], Philippa DODDS*, Augustin AMOUR*[3] and Gillian MURPHY*

*School of Biological Sciences, University of East Anglia, Norwich NR4 7TJ, U.K., †Max-Planck Institut fűr Biochemie, D-82152 Martinsried, Germany, and ‡Department of Biology, Bone and Joint Pathology, University of York, York YO10 5DD, U.K.

We previously reported that full-length tissue inhibitor of metalloproteinase-3 (TIMP-3) and its N-terminal domain form (N-TIMP-3) displayed equal binding affinity for tissue necrosis factor-α (TNF-α)-converting enzyme (TACE). Based on the computer graphic of TACE docked with a TIMP-3 model, we created a number of N-TIMP-3 mutants that showed significant improvement in TACE inhibition. Our strategy was to select those N-TIMP-3 residues that were believed to be in actual contact with the active-site pockets of TACE and mutate them to amino acids of a better-fitting nature. The activities of these mutants were examined by measuring their binding affinities (K_i^{app}) and association rates (k_{on}) against TACE. Nearly all mutants at position Thr-2 exhibited slightly impaired affinity as well as association rate constants. On the other hand, some Ser-4 mutants displayed a remarkable increase in their binding tightness with TACE. In fact, the binding affinities of several mutants were less than 60 pM, beyond the sensitivity limits of fluorimetric assays. Further studies on cell-based processing of pro-TNF-α demonstrated that wild-type N-TIMP-3 and one of its tight-binding mutants, Ser-4Met, were capable of inhibiting the proteolytic shedding of TNF-α. Furthermore, the Ser-4Met mutant was also significantly more active ($P < 0.05$) than the wild-type N-TIMP-3 in its cellular inhibition. Comparison of N-TIMP-3 and full-length TIMP-3 revealed that, despite their identical TACE-interaction kinetics, the latter was nearly 10 times more efficient in the inhibition of TNF-α shedding, with concomitant implications for the importance of the TIMP-3 C-terminal domain *in vivo*.

Key words: binding affinity, gelatinase-A, N-terminal domain of TIMP-3, TACE.

INTRODUCTION

Many bioactive proteins, including cytokines, growth factors and adhesion molecules, are synthesized as inactive transmembrane precursors that can be released into the surrounding medium upon proteolytic cleavage by specific endoproteinases. The release of these molecules, in a process termed 'shedding', has been the subject of many investigations in the past decade. Among others, the processing and maturation events surrounding tumour necrosis factor-α (TNF-α) have been the most extensively examined to date [1–3]. TNF-α is a potent pro-inflammatory cytokine produced mainly by activated monocytes and macrophages as part of the self-defence machinery. Excessive levels of TNF-α, however, have been shown to cause severe physiological disorders such as rheumatoid arthritis and Crohn's disease [4]. The enzyme responsible for TNF-α shedding was isolated in 1997 and is known as TNF-α-converting enzyme (TACE) [5,6]. Sequence analysis confirmed that TACE is a member of the zinc-dependent metalloproteases of the ADAM (a disintegrin and a metalloproteinase domain) family, and is numbered ADAM-17. The ADAM proteases are typically composed of several domains. Besides the enzymically active catalytic domain, an ADAM protease also has a N-terminal pro-domain as well as several other individual domains at its C-terminus. These C-terminal domains are commonly referred to as disintegrin, epidermal growth factor-like, crambin-like, transmembrane and cytoplasmic domains. Apart from TNF-α, TACE has also been implicated in the ectodomain shedding of many other cell-surface proteins. To name a few, L-selectin, interleukin-6 receptor, fractalkine, neuregulins and one of the isoforms of epidermal growth factor, HER-4 Jma, have all been linked to TACE-mediated shedding [7–11].

Among the four mammalian tissue inhibitors of metalloproteinases (TIMPs), only TIMP-3 has been shown to be capable of exerting significant inhibitory effects against TACE [12,13]. Crystal and NMR studies of TIMP-1 and -2 showed that TIMP molecules are folded into two very distinct domains [14–16]. The N-terminal domain comprises ≈ 120 amino acids and encompasses the first two-thirds of the TIMP molecule. Interestingly, the structure of the N-terminal domain is highly reminiscent of the oligosaccharide/oligonucleotide-binding (OB) protein motif. The C-terminal domain, on the other hand, is less structurally defined. There are three disulphide bonds in each domain, and the truncated N-terminal domains of TIMP-1, -2 and -3 have all been shown to form stable, autonomous units capable of inhibiting many matrix metalloproteinases (MMPs) and ADAMs [13,17–19].

Hitherto, only the structures of TIMP-1 and -2 have been solved [14–16]. Given the striking similarity between TIMP-1 and -2, there is little doubt that TIMP-3 should demonstrate a

Abbreviations used: TIMP, tissue inhibitor of metalloproteinase; N-TIMP-3, N-terminal domain of TIMP-3; TNF-α, tissue necrosis factor-α; TACE, TNF-α-converting enzyme; gel-A, gelatinase-A; ADAM, a disintegrin and a metalloproteinase domain; OB, oligosaccharide/oligonucleotide-binding; MMP, matrix metalloproteinase; GdmCl, guanidinium chloride; FAB fluorescence assay buffer.

[1] To whom correspondence should be addressed (e-mail meng.lee@uea.ac.uk).
[2] Present address: Department of Biology, Bone and Joint Pathology, University of York, York YO10 5DD, U.K.
[3] Present address: GlaxoSmithKline, Stevenage, Herts. SG1 2NY, U.K.

more or less comparable configuration. Efforts to refold full-length TIMP-3 from inclusion bodies have so far failed to produce significant amounts of protein for a similar study. Native TIMP-3, on the other hand, is notorious for being matrix-bound and difficult to extract even from uterine tissue, where it is known to exist in abundance [20].

In view of the versatility of TACE in the modulation of so many cell-surface molecules, many attempts have been made to synthesize specific inhibitors that could ultimately be used to regulate related pathological disorders [21]. However, none of these compounds have been demonstrated to be TACE-specific. Previously, we showed that full-length TIMP-3 and its refolded N-terminal domain (N-TIMP-3) displayed equal inhibitory affinities towards TACE [13]. Encouraged by the findings, we set out to create a new generation of 'designer' N-TIMP-3s that could bind TACE more effectively. In the present paper, we reveal that the affinity of N-TIMP-3 could indeed be strengthened substantially by substituting the appropriate amino acids at the positions where direct interactions between TIMP-3 and TACE take place.

Table 1 Oligonucleotides used in generating N-TIMP-3 mutants

The amino acids mutated in each mutant are underlined. *Nde*I and *Hin*dIII restriction sites are italicized. Rev, reverse primer.

Mutant	Oligonucleotide
Thr-2Leu	5′-GCTCAACA*CATATG*TGCCTGTGCTCGCCCAGCCACCCCCAG-3′
Thr-2Met	5′-GCTCAACA*CATATG*TGCATGTGCTCGCCCAGCCACCCCCAG-3′
Thr-2Tyr	5′-GCTCAACA*CATATG*TGCTACTGCTCGCCCAGCCACCCCCAG-3′
Ser-4Leu	5′-GCTCAACA*CATATG*TGCACATGCCTGCCCAGCCACCCCCAG-3′
Ser-4Met	5′-GCTCAACA*CATATG*TGCACATGCATGCCCAGCCACCCCCAG-3′
Ser-4Tyr	5′-GCTCAACA*CATATG*TGCACATGCTACCCCAGCCACCCCCAG-3′
Ser-4Lys	5′-GCTCAACA*CATATG*TGCACATGCAAACCCAGCCACCCCCAG-3′
Ser-4Arg	5′-GCTCAACA*CATATG*TGCACATGCCGTCCCAGCCACCCCCAG-3′
Ser-6Leu	5′-GCTCAACA*CATATG*TGCACATGCTCGCCCCTGCACCCCCAG-3′
Ser-6Met	5′-GCTCAACA*CATATG*TGCACATGCTCGCCCATGCACCCCCAG-3′
Ser-6Phe	5′-GCTCAACA*CATATG*TGCACATGCTCGCCCTTCCACCCCCAG-3′
Leu-67Phe	5′-CATACGG*AAGCTT*CCGAGAGTTTCTGTGGCCTTAAGCTGGAG-3′
Leu-67Ile	5′-CATACGG*AAGCTT*CCGAGAGTATCTGTGGCCTTAAGCTGGAG-3′
Leu-67Met	5′-CATACGG*AAGCTT*CCGAGAGTATGTGTGGCCTTAAGCTGGAG-3′
Rev	5′-CTAGTTATTGCTCAGCGGTGGCAG-3′

EXPERIMENTAL

Materials

All chemicals and reagents were purchased from Sigma (Littlehampton, West Sussex, U.K.) unless otherwise stated. Restriction enzymes and *Pwo* polymerase for PCR reactions were obtained from Roche (Mannheim, Germany). Recombinant full-length TIMP-3 and gelatinase-A (gel-A; also known as MMP-2) were purified and activated as described previously [22,23]. TACE used in this studies was a kind gift from GlaxoSmithKline Research and Development (Research Triangle Park, NC, U.S.A.) [24]. Fluorimetric substrates for gel-A (QF-24, Mca-Pro-Leu-Gly-Leu-Dpa-Ala-Arg-NH_2) and TACE [QF-45, Mca-Ser-Pro-Leu-Ala-Gln-Ala-Val-Arg-Ser-Ser-Ser-Arg-Lys-Dnp-NH_2; where Mca stands for (7-methoxycoumarin-4-yl)acetyl, Dpa stands for *N*-3-(2,4-dinitrophenyl)-L-2,3-diaminopropionyl and Dnp stands for 2,4-dinitrophenyl] assays were as mentioned in our previous paper [12]. TNF-α shedding assays were carried out using a human TNF-α ELISA kit from Cambridge Bioscience (Cambridge, U.K.). The assay of c-Met shedding was performed with A549 human lung adenocarcinoma cells obtained from the European Collection of Cell Cultures. Dulbecco's modified Eagle's medium, RPMI 1640 medium and serum for cell cultures were all purchased from Gibco BRL. A PerkinElmer LS-50B spectrofluorometer with thermostatic cuvette holders was used in kinetic studies throughout this work. All TIMPs and mutants were titrated against both TACE and gel-A to ensure accurate estimation of concentration. Pro-gel-A was activated in fluorescence assay buffer (FAB; 10 mM $CaCl_2$, 50 mM Tris/HCl, pH 7.5, 0.05 % Brij-35, 1 % DMSO and 0.02 % NaN_3) with 2 mM 4-aminophenylmercuric acid at room temperature for 1 h. Active gel-A and TACE were stored in small aliquots at -70 °C to prevent self-degradation.

N-TIMP-3 mutant constructs

All N-TIMP-3 mutants were constructed by means of PCR. The mutagenic oligonucleotides used in constructing mutants are listed in Table 1. The positions of mutated amino acids are underlined and *Hin*dIII and *Nde*I restriction sites are italicized for ease of identification. All Thr-2, Ser-4 and Ser-6 mutant cDNAs were amplified with the mutagenic oligonucleotides as forward primers. The reverse primer was a pRSET vector-specific oligonucleotide that annealed to the vector. PCR reactions were performed under the following conditions: 94 °C for 1 min, 60 °C for 30 s and 72 °C for 1 min for a total of 25 cycles. Wild-type N-TIMP-3 construct, described in our previous paper, was used as a PCR template in generating all N-TIMP-3 mutants [13]. PCR amplicons were gel-purified and double-digested with *Nde*I and *Eco*RI before being ligated into pRSET vector. Ligation mixtures were transformed into DH5α supercompetent cells and plated on to LB agar supplemented with 100 μg/ml ampicillin. After overnight incubation at 37 °C, five colonies from each mutant were chosen to be inoculated in 5 ml of 2 × YT medium with ampicillin. Cells were cultured for another 14 h at 37 °C before harvesting for Minipreps. Purified plasmids were screened by double digestion with *Nde*I and *Eco*RI restriction enzymes to confirm the presence of inserts.

Mutants from the Leu-67 series were constructed by PCR amplification of wild-type cDNA with Leu-67 forward primers (Table 1) and pRSET reverse primer. PCR amplicons were gel-purified and digested with *Hin*dIII enzyme. Digested PCR fragments were subsequently ligated into wild-type N-TIMP-3 plasmid predigested with *Hin*dIII enzyme. *Hin*dIII digestion of wild-type N-TIMP-3 plasmid released a 250 bp fragment spanning from residue 62 of N-TIMP-3 to the stop codon at the end of the cDNA insert. Only clones of correct orientations were chosen for protein expression. All DNA constructs were sequenced to confirm that no unwanted mutations had been introduced during PCR amplification.

Protein expression and purification

Escherichia coli BL21(DE3) pLys supercompetent cells were transformed with pRSET plasmids harbouring N-TIMP-3 mutant cDNAs by heat-shock at 42 °C for 45 s. Cells were plated on to LB plates supplemented with 100 μg/ml ampicillin. After overnight incubation at 37 °C, the bacterial lawns were re-suspended in 1.5 l of 2 × YT medium. When the A_{600} value reached 0.5, cells were induced with 0.5 mM isopropyl β-D-thiogalactoside. Culture were continued for a further 3 h before harvesting. Cell pellets were lysed for 30 min at 4 °C by adding lysozyme and DNase with gentle stirring. Pellets containing inclusion bodies were washed at least twice with 20 mM Tris/HCl, pH 7.5, before final centrifugation at 10000 ***g*** for 20 min. Typically, the purity of N-TIMP-3 in washed pellets was at least 80 % as judged by reducing SDS/PAGE.

Effects of pH and guanidinium chloride (GdmCl) concentrations on N-TIMP-3 mutant refolding

For analytical purposes, ≈ 100 mg of N-TIMP-3 inclusion bodies were dissolved in 3 ml of solubilization buffer (6 M GdmCl, 20 mM Tris/HCl, pH 7.5, and 10 mM dithiothreitol) for 30 min at room temperature. Insoluble proteins were discarded by centrifugation at 12000 ***g*** for 5 min. Clear supernatant (80 μl) was added to 5 ml of refolding buffer in Bijou vials containing different concentrations of GdmCl, ranging from 0 to 2 M, at three different pH values: 7.6, 8.8 and 10.0. The concentrations of oxidized and reduced glutathione (GSSG/GSH) in all refolding samples were 0.8 and 0.5 mM respectively.

Refolding was allowed to proceed at room temperature for 16 h before the samples were dialysed twice against 5 l of 50 mM Tris/HCl buffer, pH 8.0. Insoluble precipitates were removed by centrifugation at 10000 ***g*** for 5 min. In order to determine the presence of active N-TIMP-3 in the samples, 300 μl of supernatant was added to 2.2 ml of FAB containing 100 pM gel-A. The mixtures were incubated for 3 h at room temperature before adding QF-24 substrate to a final concentration of 1 μM.

The remaining activities of gel-A (rate of QF-24 proteolysis) were plotted against the concentrations of GdmCl to determine the relative amount of properly refolded N-TIMP-3 in each sample.

Effects of GSSG/GSH ratio on N-TIMP-3 refolding

N-TIMP-3 in solubilization buffer (80 μl) was added to 5 ml of refolding buffer (1.5 M GdmCl in 50 mM Tris/HCl, pH 10.0) containing different concentrations of GSSG/GSH. Six different ratios of GSSG/GSH concentrations were investigated: 0:0 mM, 0:0.8 mM, 0.25:0.8 mM, 0.5:0.8 mM, 0.5:0.4 mM and 0.5:0 mM. Refolding, dialysis and gel-A inhibition assays were essentially as described above. The activities of gel-A in each sample were plotted against GSSG/GSH ratio to determine the relative amount of active N-TIMP-3.

Preparative-scale N-TIMP-3 mutant refolding

N-TIMP-3 mutant inclusion bodies (1 g wet weight) were dissolved in 25 ml of solubilization buffer at room temperature for 30 min with constant stirring. Insoluble materials were discarded by high-speed centrifugation at 10000 ***g*** for 10 min. The supernatant was pumped into 1 l of refolding buffer consisting of 1.5 M GdmHCl in 50 mM Tris/HCl, pH 10.0, 0.8 mM GSSG and 0.2 mM GSH at the very slow speed of 1 ml/min. Refolding was performed for at least 16 h at room temperature. The following day, the refolding mixtures were dialysed twice against 30 l of 30 mM Tris/HCl, pH 8.0. Insoluble precipitates were removed by centrifugation at 12000 ***g*** for 40 min. Soluble N-TIMP-3 proteins in the supernatant were extracted with Ni^{2+}-nitrilotriacetate–agarose as described in our previous report [13]. Purified N-TIMP-3 and mutants were subjected to Western-blot analysis with anti-His-tag monoclonal antibody (Invitrogen) before kinetic assays were carried out.

Measurement of the inhibition constant (K_i^{app})

TACE (0.2 nM) and gel-A (0.1 nM) were incubated with different concentrations of N-TIMP-3 mutants, ranging from 0 to 50 nM. For the less-potent mutants (e.g. Thr-2 mutants), up to 200 nM of proteins were required in some samples. Ser-4 mutants necessitated less, with typical concentrations varying from 0 to 1.5 nM. Incubation was allowed for 3 h at room temperature prior to measurement of steady-state velocity (V_s). The final volume of incubation mixtures in K_i^{app} studies was 2.5 ml unless otherwise stated. FAB was used as the diluent throughout all kinetic studies. Quenched fluorescent peptides QF-45 and QF-24 (final concentrations, 1 μM) were used as substrates for TACE and gel-A respectively. Measurements of enzyme activities were initiated by adding substrates to incubation mixtures at 27 °C. All data were fitted to competitive tight-binding equations with the computer program Grafit to obtain an estimation of K_i^{app} values [12]:

$$V_s = (V_o/2E_t) \times \{(E_t - I_t - K_i^{app}) + [(K_i^{app} + I_t - E_t)^2 + 4E_t \cdot K_i^{app}]^{1/2}\} \quad (1)$$

where V_o is the rate in the absence of inhibitor, E_t is the total enzyme concentration and I_t is the total inhibitor concentration.

Measurement of the association rate constant (k_{on})

Measurements of k_{on} were performed by adding N-TIMP-3 mutants (10–50 nM) to TACE (0.1 nM) or gel-A (50 pM) in a final volume of 2.5 ml in FAB. The rate of inhibition was followed using a continuous fluorimetric assay at 27 °C until steady state was reached, usually after 6000–8000 s. The progress curve was analysed using the Enzfitter program (Biosoft, Cambridge, U.K.) and the equation [12]:

$$P = V_s t + (V_0 - V_s)(1 - e^{-kt})/k \quad (2)$$

where P is the product concentration, V_0 is the initial velocity and k is the apparent first-order rate constant of equilibrium between the enzyme and TIMP complex. k_{on} values were calculated by linear regression of k on TIMP concentrations. All K_i^{app} and k_{on} experiments were performed at least twice to confirm the reproducibility of the results.

Inhibition of TNF-α and c-Met shedding

TNF-α shedding was carried out using THP-1 cells cultured in 10% serum-enriched RPMI 1640 medium. For the purpose of shedding experiments, cells were washed twice with serum-free medium before being seeded into 24-well tissue-culture dishes at a density of 1.3×10^6 cells/ml. The typical volume of cells in each well was 0.5 ml. Cells were pre-incubated with increasing concentrations of full-length TIMP-3 (0.01, 0.02, 0.04, 0.07 and 0.1 μM), N-TIMP-3 (0.1, 0.2, 0.4, 0.7 and 1.0 μM) or Ser-4Met mutant (0.1, 0.2, 0.4, 0.7 and 1.0 μM) for 30 min at 37 °C before treatment with PMA (50 ng/ml) to induce shedding. After incubation for a further 4 h, the supernatants were harvested and used in a subsequent ELISA assay.

The procedures of ELISA were essentially as described in the brochure accompanying the kit. Samples were assayed at four different dilutions in duplicate in order to confirm the validity of the results. The reproducibility of TIMP-3 inhibitory effects on TNF-α shedding was ascertained by repeating the experiment at least twice on different batches of THP-1 cells. Student's t test was used to verify the significance between the wild-type and the Ser-4Met mutant data.

The shedding of c-Met, on the other hand, was measured with A549 cells at a density of 4×10^5 cells/well in serum-free Dulbecco's modified Eagle's medium. Full-length N-TIMP-3 or Ser-4Met mutant (0.1–0.3 μM) were added to cells for 30 min before induction with PMA (20 ng/ml). Supernatants from each sample were collected 6 h post-induction and concentrated 10-fold with a Centricon-10 concentrator (Amicon). The presence of soluble c-Met was detected by Western-blot analysis using the DL-21 monoclonal antibody (1:2500; Upstate Biotechnology, Lake Placid, NY, U.S.A.) at 4 °C for 16 h followed by horseradish

peroxidase-conjugated sheep anti-mouse monoclonal antibody (1:5000) for 1 h at room temperature.

Computer modelling

EXPASY Molecular Biology Server, WebLab ViewerLite and Rasmol programs were used for three-dimensional modelling. The inter-atomic distances in TACE active sites were calculated using Rasmol.

RESULTS

The effects of mutagenesis on N-TIMP-3 refolding

Although full-length TIMP-3 has not been refolded successfully, N-TIMP-3 refolding is relatively straightforward. Previously, we adopted 0.45 M as the concentration of GdmCl for refolding recombinant N-TIMP-3 protein [13]. During the course of this study, we performed a series of screening assays and found that 1.5 M GdmCl was the ideal concentration. Although the yield of active N-TIMP-3 was not as high as those for N-TIMP-1 and -2, the recovery rate was typically 5 % of the starting materials. As illustrated in Figure 1, the yield of active N-TIMP-3 increased substantially under very basic and oxidized conditions (pH 10.0 and a GSSG/GSH ratio of 0.5:0 mM). The isoelectric point (pI) of N-TIMP-3 polypeptide was calculated to be 8.8 while the pK_a value of an isolated cysteine group is ≈ 8.6 (EXPASY Molecular Biology Server). Thus we expect most cysteine residues to be ionized under the refolding conditions described above. Such a basic environment would almost certainly accelerate the shift of equilibrium towards the formation of intra-molecular disulphide bonds.

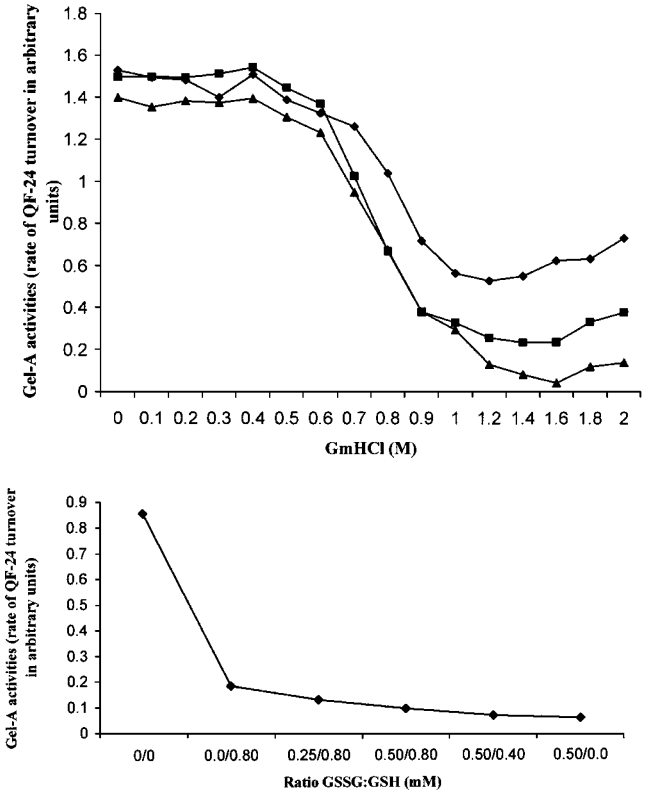

Figure 1 (Top panel) The effects of GdmCl on N-TIMP-3 refolding and (bottom panel) the effects of GSSG/GSH ratio on N-TIMP-3 refolding

Top panel: equal volumes of solubilized N-TIMP-3 were added to 5 ml of refolding solution containing different concentrations of GdmCl. The *y*-axis represents the activities of remaining gel-A after 3 h of incubation with 300 μl of dialysed N-TIMP-3 refolding solution. ◆, Refolding at pH 7.5; ■, refolding at pH 8.8; ▲, refolding at pH 10.0. Bottom panel: the activities of gel-A after 3 h of incubation are plotted (*y*-axis) against the ratio of GSSG/GSH (*x*-axis).

Table 2 K_i^{app} of N-TIMP-3 and its mutants with TACE and gel-A

u, Mutants that were unable to refold using the refolding conditions developed in this laboratory.

	K_i^{app} (nM)	
	Gel-A	TACE
Full-length TIMP-3*	< 0.002	0.2 ± 0.03
N-TIMP-3*	0.25 ± 0.05	0.22 ± 0.07
Thr-2Leu	2.1 ± 0.12	0.49 ± 0.07
Thr-2Met	0.29 ± 0.02	0.77 ± 0.06
Thr-2Tyr	49.0 ± 5.8	1.3 ± 0.16
Ser-4Leu	6.3 ± 1.75	0.066 ± 0.016
Ser-4Met	3.18 ± 0.07	< 0.06
Ser-4Tyr	3.03 ± 0.23	0.063 ± 0.012
Ser-4Lys	2.77 ± 0.05	< 0.06
Ser-4Arg	4.91 ± 0.31	< 0.06
Ser-6Leu	u	u
Ser-6Met	u	u
Ser-6Phe	u	u
Leu-67Phe	u	u
Leu-67Ile	u	u
Leu-67Met	1.32 ± 0.05	0.073 ± 0.014

* Data published in [13].

We extended the same refolding conditions to all Thr-2 and Ser-4 mutants with apparent success. The yield of active proteins from the Thr-2 and Ser-4 mutant series was comparable with that of the wild-type N-TIMP-3. Most interestingly, replacement of the Ser-4 residue by positively charged amino acids (lysine/arginine) had no adverse effects on the refolding efficiency. On the contrary, all Ser-6 and Leu-67Phe/Ile mutants were not refoldable despite using the same method. Repeated attempts to refold Ser-6 and Leu-67Phe/Ile mutants under modified conditions as reported by Kashiwagi et al. [25] also failed to produce enough protein for kinetic analysis (results not shown).

Studies of binding affinity (K_i^{app})

Thr-2 → Leu/Met/Tyr mutants

The amino acids chosen to substitute Thr-2 were dependent solely on the unique environment of the S1′ crevice of the TACE enzyme [26]. A rough calculation on our computer model showed that the S1′ cavity is ≈ 5.5–6.0 Å in depth and seemingly very hydrophobic in nature. The length of the threonine side chain, on the other hand, is less than 2.5 Å. Thus we decided to lengthen the position 2 residue by replacing threonine with amino acids of longer side chains. Leucine, methionine and tyrosine were chosen as replacements largely because they fulfilled the criteria of being bulkier than threonine and were therefore most likely to extend deeper into the S1′ pocket.

Our kinetic data showed that, instead of strengthening the interactions with TACE, the binding affinity of all Thr-2 mutants actually decreased modestly (Table 2). The K_i^{app} value of 0.5–1.3 nM was slightly higher than those of the wild-type protein (K_i^{app}, 0.2 nM). Not surprisingly, the reduction in binding affinity with gel-A was even more dramatic. In fact, all mutants

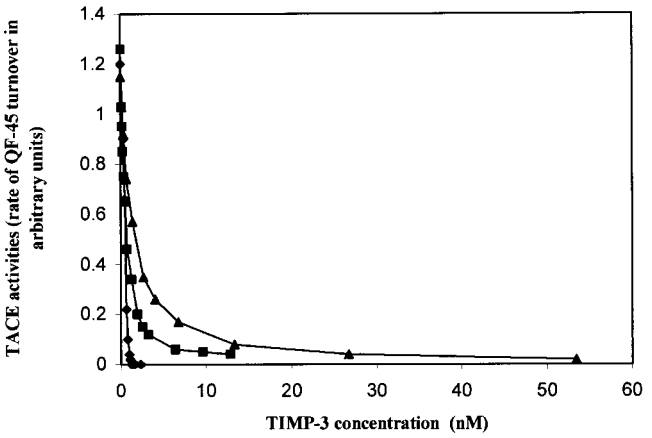

Figure 2 The K_i^{app} inhibition profiles of wild-type N-TIMP-3 (■), Thr-2Tyr (▲) and Ser-4Met mutants (◆) with TACE

Ser-4Met has such high affinity that, at concentrations higher than 1.0 nM, TACE was completely inactivated. Thus no K_i^{app} value could be calculated from the Ser-4Met curve. K_i^{app} values were as follows: wild-type N-TIMP-3, 0.2 nM; Thr-2Tyr, 1.3 nM; Ser-4Met mutants, < 60 pM.

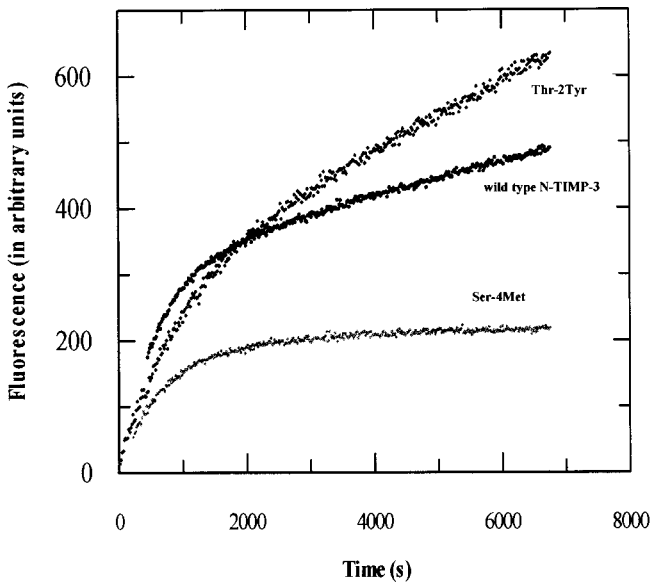

Figure 3 The k_{on} inhibition profiles of wild-type N-TIMP-3, Thr-2Tyr and Ser-4Met mutants against TACE

Wild-type (2.5 nM), Thr-2Tyr (2.8 nM) and Ser-4Met mutants (2.4 nM) were added to TACE (0.15 nM) in 2.5 ml cuvettes in the presence of 1 μM QF-45 substrate. At equilibrium, TACE was much less active in the Ser-4Met sample than in those of the wild-type or Thr-2Tyr mutant. Also, smaller amounts of Ser-4Met were required to demonstrate complete inhibition of TACE. The y-axis represents the turnover of QF-45 substrate (fluorescence in arbitrary units).

constructed in this work were expected to be very poor inhibitors for gel-A because of the simple fact that the side chains chosen were too long for the gel-A S1′ and S3′ cavities.

Ser-4 → Leu/Met/Tyr mutants

Crystallography data on the active cleft of TACE revealed that, among others, the S1′ specificity pocket was fused with the neighbouring S3′ pocket under the surface of the enzyme [26]. In addition, the active-site cleft becomes slightly 'notched' towards the very prime end of the molecule. The S3′ pocket shares the same fundamental physical properties as its S1′ neighbour, except that the cavity is even deeper and larger in size. Hindered by the uncertainty surrounding the actual binding site in the pocket, we estimated the cavity to be at least 7.0–8.0 Å in depth. Hence, in comparison with the volume of the cavity it is supposed to occupy, the size of the TIMP-3 Ser-4 side chain appeared to be very minute indeed.

The criteria for the selection of amino acids to replace the Ser-4 residue were analagous with those for S1′ pocket. Indeed, our kinetic findings confirmed that all Ser-4Leu/Met/Tyr mutants did demonstrate remarkable improvement in binding affinity with TACE, as predicted by the crystallographic model (Table 2). The K_i^{app} values of Ser-4Leu and Ser-4Tyr mutants varied between 60 and 70 pM, close to the sensitivity limit of our fluorimetric assays. Especially noteworthy is the Ser-4Met mutant; its binding affinity with TACE was so strong that the K_i^{app} value could not be determined accurately (Figure 2). Repeated attempts to measure the K_i^{app} values using different enzyme concentrations were also unsuccessful, mainly due to the non-dissociating manner of Ser-4Met binding. As a matter of fact, the enzyme was completely inactivated by the Ser-4Met mutant at the molar ratio of 1:5 (enzyme/inhibitor) in a 2.5 ml assay cuvette. Figure 2 demonstrates the inhibitory profiles of wild-type N-TIMP-3 (K_i^{app}, 0.2 nM) with TACE. Thr-2Tyr (K_i^{app}, 1.3 nM) and Ser-4Met (K_i^{app}, < 0.06 nM) mutants are included in Figure 2 for comparison. In the case of a poor mutant (Thr-2Tyr), considerably more protein was required. In contrast, Ser-4Met completely inactivated TACE at 1 nM. The k_{on} profiles of wild-type N-TIMP-3, Thr-2Tyr and Ser-4Met are shown as time courses in Figure 3. Most interestingly, TACE was completely inhibited by Ser-4Met at equilibrium but not by wild-type N-TIMP-3 or the Thr-2Tyr mutant.

As anticipated, all Ser-4 mutants have impaired binding with gel-A, an observation clearly reflected in their high K_i^{app} values.

Ser-4 → Lys/Arg mutants

Although the TACE active site exhibits the general feature of hydrophobicity, we noted a unique Glu-398 residue at the far edge of the S3′ cleft. The side chain of this glutamic acid seems to be pointing towards the S3′ cavity; moreover, it does not form any hydrogen bond with the surrounding amino acids. The carboxylic group of Glu-398 is estimated to be ≈ 7.5 Å from a bound N-TIMP-3 model. If a suitable residue could be found to establish an electrostatic bond with this carboxylate group, the binding tightness of the resultant N-TIMP-3 mutant would be substantially enhanced. We therefore decided to also create lysine and arginine mutants at the position of Ser-4. Results from the binding studies confirm the formation of a very tight complex between Ser-4Lys/Arg and TACE, the K_i^{app} of these mutants being lower than 60 pM (the sensitivity limit of our fluorimetric assay).

Leu-67 → Met mutant

Leu-67 is situated at position P2 on the non-primed side of the catalytic zinc. In TIMP-1 and -2, the amino acid valine replaces leucine at this locus. Although there is no deep pocket on the surface of TACE that interacts with this residue, the P2–S2 interaction is predicted to be important in determining the specificity of TIMP-3. Our data showed that there was indeed a

Table 3 Association rate constants (k_{on}) of N-TIMP-3 and its mutants towards TACE and gel-A

u, Mutants that were unable to refold.

	k_{on} ($\times 10^5$ $M^{-1} \cdot s^{-1}$)	
	Gel-A	TACE
Full-length TIMP-3*	> 100	9.94 ± 0.46
N-TIMP-3*	0.25 ± 0.06	3.65 ± 0.33
Thr-2Leu	1.4 ± 0.18	1.12 ± 0.05
Thr-2Met	2.81 ± 0.81	3.34 ± 1.01
Thr-2Tyr	0.015 ± 0.005	0.48 ± 0.05
Ser-4Leu	0.48 ± 0.05	2.66 ± 0.04
Ser-4Met	0.28 ± 0.01	3.0 ± 0.42
Ser-4Tyr	0.19 ± 0.02	2.71 ± 0.02
Ser-4Lys	0.29 ± 0.11	3.12 ± 0.22
Ser-4Arg	0.31 ± 0.03	1.84 ± 0.19
Ser-6Leu	u	u
Ser-6Met	u	u
Ser-6Phe	u	u
Leu-67Phe	u	u
Leu-67Ile	u	u
Leu-67Met	0.73 ± 0.04	2.96 ± 1.44

* Data published in [13].

significant increase in binding affinity. The K_i^{app} value of 73 pM was barely within the measurable limit of our assays.

Studies of the association rate constant (k_{on})

Thr-2 → Leu/Met/Tyr mutants

The association rate constant (k_{on}) is the reflection of the speed of interactions between N-TIMP-3 and TACE in forming a stable binary complex. Thr-2Leu and Thr-2Met mutants showed little or no significant alteration in their k_{on} values [(1–3) $\times 10^5$ $M^{-1} \cdot s^{-1}$] with TACE (Table 3). However, the rate was considerably lower in Thr-2Tyr mutant (0.5×10^5 $M^{-1} \cdot s^{-1}$). It is tempting to postulate that the tyrosine side chain was too long for the S1′ specificity pocket, hence the reduction in association rate.

Ser-4 → Leu/Met/Tyr/Lys/Arg mutants

Despite the remarkable increase in binding affinity, all Ser-4 mutants displayed equal k_{on} values with TACE, suggesting no genuine discrepancy in their association rates (Table 3). Even the Ser-4Lys/Arg mutants had k_{on} rates that were indistinguishable from their wild-type counterparts.

Leu-67 → Met mutant

The k_{on} data for this mutant also showed no improvement in the association rate with the TACE enzyme. The value of 3.0×10^5 $M^{-1} \cdot s^{-1}$ was very similar to the wild-type value (3.6×10^5 $M^{-1} \cdot s^{-1}$).

Inhibition of TNF-α and c-Met shedding by full-length TIMP-3, N-TIMP-3 and Ser-4Met

In order to compare the potency of N-TIMP-3 and its derivatives in inhibiting putative ADAM proteases on the cell surface, we subjected full-length TIMP-3, wild-type N-TIMP-3 and one of its tight-binding mutants, Ser-4Met, to TNF-α and c-Met shedding assays. It is well documented that pro-TNF-α is proteolytically processed by TACE, whereas the exact ADAM

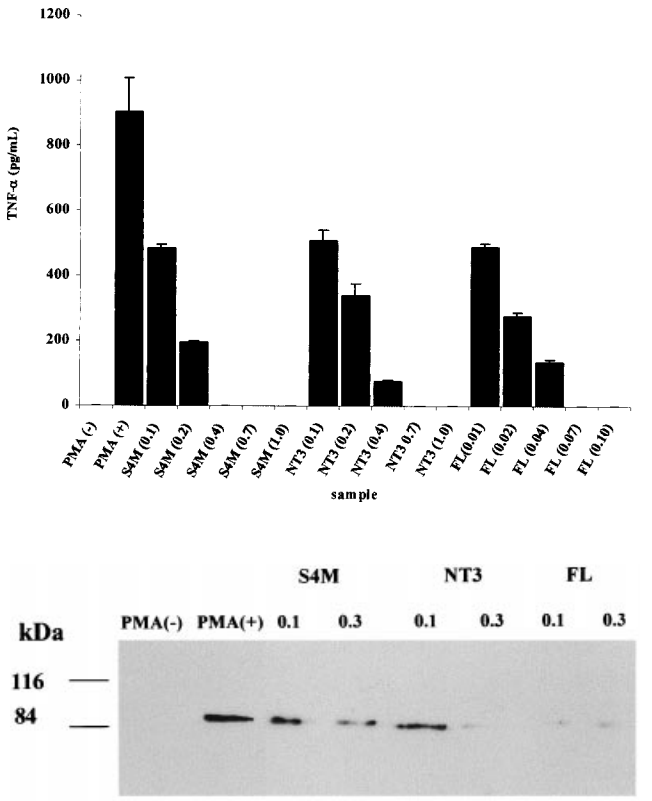

Figure 4 (Top panel) ELISA analysis of TNF-α shedding with THP-1 monocytic cells and (bottom panel) Western-blot analysis of c-Met shedding

Top panel: cells were pre-incubated with the indicated concentrations of Ser-4Met (S4M; 0.1–1.0 μM), N-TIMP-3 (NT3; 0.1–1.0 μM) or full-length TIMP-3 (FL; 0.01–0.1 μM) for 30 min prior to PMA induction (50 ng/ml). After 4 h incubation, the media were harvested for ELISA assay as described in the Experimental section. PMA(−), negative control in which no PMA was added to the medium in order to monitor the basal shedding levels of THP-1 cells; PMA(+), positive control without TIMP-3 pre-incubation. Bottom panel: A549 cells were treated with Ser-4Met mutant, N-TIMP-3 or full-length TIMP-3 (all 0.1 and 0.3 μM) for 30 min before stimulation with PMA (20 ng/ml). PMA(+), positive control without TIMP-3 pre-incubation before PMA stimulation; PMA(−), unstimulated cells. Medium from each sample was concentrated 10-fold and analysed by Western blotting using the DL-21 monoclonal antibody against c-Met.

responsible for the shedding of c-Met, the receptor for the hepatocyte growth factor, has not been identified. However, work from our laboratory has demonstrated previously that the shedding of c-Met is also mediated by a TIMP-3-sensitive metalloproteinase [27].

As shown in Figure 4 (top panel), full-length TIMP-3 completely inhibits TNF-α shedding at concentrations as low as 0.07 μM. To achieve a similar effect, significantly more wild-type N-TIMP-3 was required (0.7 μM). The Ser-4Met mutant, however, was needed at the slightly lower level of 0.4 μM to achieve complete inhibition. Statistical analysis suggests that the Ser-4Met mutant was significantly more effective than the wild-type N-TIMP-3 ($P < 0.05$). Noticeably, neither species of N-TIMP-3 was as potent as the full-length TIMP-3 in inactivating ADAM proteases on the cell surface. In the case of c-Met-shedding inhibition, the inhibitory effects of full-length TIMP-3 were also absolute at 0.1 μM (Figure 4, bottom panel). N-TIMP-3 and the Ser-4Met mutant were required at significantly higher concentrations (at least 0.3 μM) to abolish the shedding entirely.

DISCUSSION

Members of the ADAM family are now known to be implicated in the progress and aetiology of many pathological disorders ranging from rheumatoid arthritis to cancer cachexia, yet we are still no closer to regulating the activities of this class of zinc-dependent proteases. In spite of the impressive armoury of hydroxamate-based MMP inhibitors reported in the literature, none of these compounds are considered to be genuinely TACE-specific.

Hitherto, only TIMP-3 has been shown to be inhibitory towards TACE [12,13]. There is every indication to suggest that TIMP-3, but not TIMP-1 and -2, is the member of the TIMP family that could potentially play a role in the modulation of ADAMs [12,28–31]. For this reason, it is reasonable to consider TIMP-3 as the basis of new therapeutic approaches to diseases in which ADAMs have been implicated.

Full-length TIMP-3 is notoriously difficult to refold from inclusion bodies. As yet, there have been no reports of any success with the refolding of this protein. Our previous paper on TIMP-3 demonstrated that the refolded N-terminal domain of TIMP-3 displayed equal binding affinity against TACE versus its full-length counterpart [13]. Thus it appears that under *in vitro* conditions, the C-terminal domain is not essential for TACE binding. Since N-TIMP-3 is much more amenable to refolding, it seems to be the ideal target for the engineering of a TACE-specific inhibitor.

TACE is the only ADAM successfully crystallized and studied in detail to date [26]. Close scrutiny of its distinctive active cleft does support the possibility of making 'designer' forms of TIMP-3, which could in theory bind to TACE with increased affinity. Nevertheless, due to the lack of TIMP-3–TACE co-crystal structure, we could only postulate that the Thr-2 side chain of N-TIMP-3 might interact with TACE via hydrogen bonding with the active-site glutamate residue (Glu-406). Here, our findings with Thr-2 mutants illustrated that simply extending the residue to fit 'snugly' into the S1′ specificity pocket might not be the right strategy. Even though the Thr-2 side chain looked relatively small compared with the size of the pocket it occupied, it was clearly a superior residue relative to leucine, methionine or tyrosine, all of which are supposed to fit into the S1′ pocket more 'snugly'. Rather, TIMP-3 and TACE must interact in a more subtle and complicated manner. So far, we could not rule out the possibility that the Thr-2 residue of TIMP-3 might have to induce some kind of conformational changes in the S1′ pocket, and this seemingly undersized residue is the best suited amino acid to do so.

The S3′ pocket appeared to be much larger and deeper in size than the S1′ pocket [26]. As mentioned above, we are not certain of the exact role of the Glu-398 residue situated at the end of the pocket. All Ser-4 mutants exhibited augmented binding affinity, although Ser-4Met/Lys/Arg were particularly efficacious. Irrefutably, the enhanced affinity displayed by Ser-4Leu/Met/Tyr mutants against TACE was a direct result of the increased hydrophobicity as well as the length of the side chain. On the other hand, Ser-4Lys/Arg mutants were constructed with the Glu-398 residue in mind. In spite of the fact that their K_i^{app} values were beyond accurate measurement, the k_{on} data, however, suggested no real acceleration in the process of inhibition.

The interaction between TACE and TIMP is known to be a multi-step process in which TIMP (I) is thought to dock into the active site of TACE (E) in at least two phases [32]:

$$E + I \underset{k_{-1}}{\overset{\text{fast } k_1}{\leftrightarrow}} EI^* \overset{\text{slow } k_2}{\rightarrow} EI \qquad (3)$$

The first phase involves a brief millisecond enzyme–inhibitor encounter to form a loose binary complex, EI*. Subsequently, both the enzyme and TIMP undergo very strenuous conformational changes before a tight, stable complex EI can be brought into being. The second phase can take hours and is generally considered to be the rate-limiting step of TIMP–TACE interaction. Given the lack of improvement in association rate observed in the Ser-4Lys/Arg mutants, we are not certain if electrostatic bonding with the Glu-398 residue was in fact established. If the substitution of Ser-2 by Lys and Arg only accelerated the first phase (k_1) and not the second (k_2), there would indeed be no overall increase in k_{on} value. Attempts to clarify the question further by measuring K_i^{app} in the presence of salt were unsuccessful due to the fact that TACE is highly sensitive to NaCl [24]. In fact, TACE was shown in our laboratory to be only 20 % active if 150 mM NaCl was added to the assay buffer (results not shown).

Unlike mutations at position Thr-2 and Ser-4, all mutants at position Ser-6 were intractable to refolding. In addition to the refolding protocol developed in this laboratory, we also attempted the alternative method reported by Kashiwagi et al. [25], but to no avail. The Ser-6 residue is situated right after the proline-5 'kink' where the TIMP-3 polypeptide turns into its first α-loop. Our modelling hinted that the side chain of Ser-6 was buried firmly in the OB fold of the N-TIMP-3 molecule. Any expansion of this side chain would inevitably disrupt the integrity of the OB core. On the other hand, it is hard to explain the inability of Leu-67Phe and Leu-67Ile mutants to refold. Computer modelling showed that the Leu-67 residue was pointed away from the OB core. During the process of refolding, we repeatedly noted that the yield of Leu-67Met mutant was considerably less than that of the wild-type N-TIMP-3. Collectively, our experience suggests that Leu-67 plays a key role in the refolding pathway of N-TIMP-3 polypeptide.

Most excitingly, our results prove that N-TIMP-3 was entirely capable of inhibiting TNF-α shedding. This is the first time that refolded N-TIMP-3 was reported to be effective against native TACE enzyme on the cell surface. Interestingly, statistical analysis on the shedding data also complements our kinetic observations in that the tight-binding mutant, Ser-4Met, was indeed significantly more active than the wild-type N-TIMP-3 ($P < 0.05$).

In comparison with the full-length species, however, almost 6–10-fold more Ser-4Met or N-TIMP-3 was required to demonstrate total inhibition of TNF-α shedding. At present, we cannot rule out the likelihood that the C-terminal domain of TIMP-3 could play a significant role in the association of the molecule into the extracellular matrix. That is, full-length TIMP-3 was shown to be more active against TACE simply because it was sequestered at the extracellular matrix where TACE is also present in close proximity, and it is this togetherness that brought about the observed higher potency of full-length TIMP-3. To date, the role of the TIMP-3 C-terminal domain is still largely shrouded in controversy. Langton et al. [33] presented evidence that the C-terminal domain was responsible for the unique matrix-binding features of TIMP-3. In their studies, truncated TIMP-3 (N-TIMP-3) expressed in mammalian cells was found exclusively in the medium instead of being matrix-bound. On the other hand, contradictory findings by Yu et al. [20] suggested that the heparin-binding sequences of TIMP-3 resided mainly at the N-terminus. It seems reasonable to assume that these 'heparin-binding sequences' are, in fact, responsible for the matrix-binding characteristics of TIMP-3. In essence, more comprehensive research into the C-terminal domain is imperative before its functions can be revealed unambiguously.

Here we describe an exciting frontier in the development of a novel class of TACE inhibitors. Our findings have made clear the possibility of engineering a new generation of N-TIMP-3 molecules that could target TACE more selectively. We are currently in the process of co-crystallizing TACE with some of the tight-binding mutants in order to unveil the exact interactions between TIMP-3 and TACE molecules. On the other hand, our findings also highlighted the uncertainties surrounding the precise functions of the C-terminal domain of the TIMP-3 molecule. Unlocking the secret of TIMP-3–TACE interactions would undoubtedly have a profound repercussion in the treatment of ADAM-related pathological diseases in the future.

This work was supported by the Arthritis Research Campaign, Medical Research Council, Wellcome Trust and Biotechnology and Biological Sciences Research Council of the U.K. We thank Mr G. Vogt for excellent technical assistance throughout this work. Thanks also to Dr R. Williamson of the University of Kent in Canterbury for expert advice on protein refolding and optimization.

REFERENCES

1 Gearing, A. J. H., Beckett, P., Christodoulou, M., Churchill, M., Clements, J., Davidson, A. H., Drummond, A. H., Galloway, W. A., Gilbert, R., Gordon, J. L. et al. (1994) Matrix metalloproteinases and processing of pro-TNF-α. Nature (London) **370**, 555–557

2 McGeehan, G. M., Becherer, J. D., Bast, R. C., Boyer, C. M., Champion, B., Connolly, K. M., Conway, J. G., Furdon, P., Karp, S., Kidao, S. et al. (1994) Regulation of tumour necrosis factor-α processing by a metalloproteinase inhibitor. Nature (London) **370**, 558–561

3 Black, R. A., Durie, F. H., Otten-Evans, C., Miller, R., Slack, J. L., Lynch, D. H., Castner, B., Mohler, K. M., Gerhart, M., Johnson, R. S. et al. (1996) Relaxed specificity of matrix metalloproteinases (MMPs) and TIMP insensitivity of tumor necrosis factor-α (TNF-α) production suggest the major TNF-α converting enzyme is not an MMP. Biochem. Biophys. Res. Commun. **225**, 400–405

4 Beutler, B. and Cerami, A. (1988) Tumor necrosis, cachexia, shock and inflammation: a common mediator. Annu. Rev. Biochem. **57**, 505–518

5 Black, R. A., Rauch, C. T., Kozlosky, C. J., Peschon, J. J., Slack, J. L., Wolfson, M. F., Castner, B. J., Stocking, K. L., Reddy, P., Srinivasan, S. et al. (1997) A metalloproteinase disintegrin that releases tumor-necrosis factor-α from cells. Nature (London) **385**, 729–732

6 Moss, M. L., Jin, S. L. C., Milla, M. E., Burkhart, W., Carter, H. L., Chen, W. J., Clay, W. C., Didsbury, J. R., Hassler, D., Hoffman, C. R. et al. (1997) Cloning of a disintegrin metalloproteinase that processes precursor tumour-necrosis factor-α. Nature (London) **385**, 733–736

7 Borland, G., Murphy, G. and Ager, A. (1999) Tissue inhibitor of metalloproteinases-3 inhibits shedding of L-selectin from leukocytes. J. Biol. Chem. **274**, 2810–2815

8 Hargreaves, P. G., Wang, F. F., Antcliff, J., Murphy, G., Lawry, J., Graham, R., Russell, G. and Croucher, P. I. (1998) Human myeloma cells shed the interleukin-6 receptor: inhibition by tissue inhibitor of metalloproteinase-3 and hydroxamate-based metalloproteinase inhibitor. Br. J. Haematol. **101**, 694–702

9 Garton, K. J., Gough, P. J., Blobel, C. P., Murphy, G., Greaves, D. R., Dempsey, P. J. and Raines, E. W. (2001) Tumour necrosis factor-α converting enzyme (ADAM-17) mediates cleavage and shedding of fractalkine (CX3CL1). J. Biol. Chem. **276**, 37993–38001

10 Montero, J. C., Yuste, L., Diaz-Rodriguez, E., Esparis-Ogando, A. and Pandiella, A. (2000) Differential shedding of transmembrane neuregulin isoforms by the tumor necrosis factor-α converting enzyme. Mol. Cell. Neurosci. **16**, 631–648

11 Rio, C., Buxbaum, J. D., Peschon, J. J. and Corfas, G. (2000) Tumor necrosis factor-α converting enzyme is required for cleavage of erbB4/HER4. J. Biol. Chem. **275**, 10379–10387

12 Amour, A., Slocombe, P. M., Webster, A., Butler, M., Knight, C. G., Smith, B. J., Stephens, P. E., Shelly, C., Hutton, M., Knäuper, V. et al. (1998) TNF-α converting enzyme (TACE) is inhibited by TIMP-3. FEBS Lett. **435**, 39–44

13 Lee, M. H., Knäuper, V., Becherer, J. D. and Murphy, G. (2001) Full-length and N-TIMP-3 display equal inhibitory activities towards TNF-α convertase. Biochem. Biophys. Res. Commun. **280**, 945–950

14 Wu, B., Arumugam, S., Gao, G., Lee, G., Semenchenko, V., Huang, W., Brew, K. and Van Doren, S. R. (2000) NMR structure of tissue inhibitor of metalloproteinases-1 implicates localized induced fit recognition of matrix metalloproteinases. J. Mol. Biol. **295**, 257–268

15 Tuuttila, A., Morgunova, E., Bergmann, U., Lindqvist, Y., Maskos, K., Fernandez-Catalan, C., Bode, W., Tryggvason, K. and Schneider, G. (1998) Three-dimensional structure of human tissue inhibitor of metalloproteinases-2 at 2.1 Å resolution. J. Mol. Biol. **284**, 1133–1140

16 Muskett, F. W., Frenkiel, T. A., Feeney, J., Freedman, R. B., Carr, M. D. and Williamson, R. A. (1998) High resolution structure of the N-terminal domain of tissue inhibitor of metalloproteinases-2 and characterization of its interaction site with matrix metalloproteinase-3. J. Biol. Chem. **273**, 21736–21743

17 Murphy, G., Houbrechts, A., Cockett, M. I., Williamson, R. A., O'Shea, M. and Docherty, A. J. P. (1991) The N-terminal domain of tissue inhibitor of metalloproteinases retains metalloproteinase inhibitory activity. Biochemistry **30**, 8097–8102

18 Nguyen, Q., Willenbrock, F., Cockett, M. I., O'Shea, M., Docherty, A. J. P. and Murphy, G. (1994) Different domain interactions are involved in the binding of tissue inhibitors of metalloproteinases to stromelysin-1 and gelatinase A. Biochemistry **33**, 2089–2095

19 Butler, G. S., Hutton, M., Wattam, B. A., Williamson, R. A., Knäuper, V., Willenbrock, F. and Murphy, G. (1999) The specificity of TIMP-2 for matrix metalloproteinases can be modified by single amino acid mutations. J. Biol. Chem. **274**, 20391–20396

20 Yu, W. H., Yu, S. C., Meng, Q., Brew, K. and Woessner, J. F. (2000) TIMP-3 binds to sulfated glycosaminoglycans of the extracellular matrix. J. Biol. Chem. **275**, 31226–31232

21 Greenwald, R. A., Zucker, S. and Golub, L. M. (eds) (1999) Inhibition of matrix metalloproteinases, therapeutic applications. Special issue. Ann. N.Y. Acad. Sci. **878**

22 Apte, S. S., Olsen, B. R. and Murphy, G. (1995) The gene structure of tissue inhibitor of metalloproteinases (TIMP)-3 and its inhibitory activities define the distinct TIMP gene family. J. Biol. Chem. **270**, 14313–14318

23 Murphy, G., Willenbrock, F., Ward, R. V., Cockett, M. I., Eaton, D. and Docherty, A. J. P. (1992) The C-terminal domain of 72 kDa gelatinase A is not required for catalysis, but is essential for membrane activation and modulates interactions with tissue inhibitors of metalloproteinases. Biochem. J. **283**, 637–641

24 Milla, M. E., Leesnitzer, M. A., Moss, M. L., Clay, W. C., Carter, H. L., Miller, A. B., Su, J. L., Lambert, M. H., Willard, D. H., Sheeley, D. M. et al. (1999) Specific sequence elements are required for the expression of functional tumor necrosis factor α-converting enzyme (TACE). J. Biol. Chem. **274**, 30563–30570

25 Kashiwagi, M., Tortorella, M., Nagase, H. and Brew, K. (2001) TIMP-3 is a potent inhibitor of aggrecanase-1 (ADAM-TS4) and aggrecanase-2 (ADAM-TS5). J. Biol. Chem. **276**, 12501–12504

26 Maskos, K., Fernandez-Catalan, C., Huber, R., Bourenkov, G. P., Bartunik, H., Ellestad, G. A., Reddy, P., Wolfson, M. F., Rauch, C. T., Castner, B. J. et al. (1998) Crystal structure of the catalytic domain of human tumour necrosis factor-α-converting enzyme. Proc. Natl. Acad. Sci. U.S.A. **95**, 3408–3412

27 Nath, D., Williamson, N. J., Jarvis, R. and Murphy, G. (2001) Shedding of c-met is regulated by crosstalk between a G-protein coupled receptor and the EGF receptor and is mediated by a TIMP-3 sensitive metalloproteinase. J. Cell Sci. **114**, 1213–1220

28 Amour, A., Knight, C. G., Webster, A., Slocombe, P. M., Stephens, P. E., Knäuper, V., Docherty, A. J. P. and Murphy, G. (2000) The *in vitro* activity of ADAM-10 is inhibited by TIMP-1 and TIMP-3. FEBS Lett. **473**, 275–279

29 Fitzgerald, M. L., Wang, Z., Park, P. W., Murphy, G. and Bernfield, M. (2000) Shedding of syndecan-1 and -4 ectodomains is regulated by multiple signaling pathways and mediated by a TIMP-3 sensitive metalloproteinase. J. Cell Biol. **148**, 811–824

30 Loechel, F., Fox, J. W., Murphy, G., Albrechtsen, R. and Wewer, U. M. (2000) ADAM-12S cleaves IGFBP-3 and IGFBP-5 and is inhibited by TIMP-3. Biochem. Biophys. Res. Commun. **278**, 511–515

31 Wei, P., Zhao, Y. G., Zhuang, L., Ruben, S. and Sang, Q. X. A. (2001) Expression and enzymatic activity of human disintegrin and metalloprteinase ADAM 19/meltrin-β. Biochem. Biophys. Res. Commun. **280**, 744–755

32 Williams, J. W., Morrison, J. F. and Duggleby, R. G. (1979) Methotrexate, a high affinity pseudosubstrate of dihydrofolate reductase. Biochemistry **18**, 2567–2573

33 Langton, K. P., Barker, M. D. and McKie, N. (1998) Localization of the functional domains of human tissue inhibitor of metalloproteinase-3 and the effects of a Sorby's fundus dystrophy mutation. J. Biol. Chem. **273**, 16778–16781

Received 10 December 2001/4 February 2002; accepted 27 February 2002